

Analyzing Yengisogat Glacier surface velocities with ALOS PALSAR data feature tracking, Karakoram, China

Zong-li Jiang · Shi-yin Liu · Juliane Peters ·
Jian Lin · Si-chun Long · Yong-shun Han ·
Xin Wang

Received: 11 June 2010 / Accepted: 12 January 2012 / Published online: 31 January 2012
© Springer-Verlag 2012

Abstract Little is known about the detailed behavior of glaciers in the Karakoram Mountains. Advanced land observing satellite (ALOS) phased array type L-band synthetic aperture radar (PALSAR) data were used to obtain the surface velocity of the Yengisogat Glacier in the Karakoram Mountains. Four ALOS PALSAR data sets with 46 days temporal baseline acquired from 2007 to 2009 covered all four seasons and were used to extract the offset fields and estimate annual average surface velocity based on seasonal velocities. For the ALOS PALSAR data the synthetic aperture radar (SAR) feature-tracking procedures within the GAMMA software were utilized instead of SAR interferometry because of low coherence in case of fast-moving glaciers or large time intervals between the image acquisitions. The accuracy of the measurements is discussed, and the measurements were consistent with previous results from optical imagery feature tracking. It was revealed that the south tributaries contributed to the main flow of the glacier, with the glacier surface velocities of the south tributaries moving more rapidly than the north tributaries. This was

mainly attributed to the effect of the glacier's aspect in the glacier long-term development point of view. Seasonal and spatial variations of the glacier surface velocity imply that the tributary South Skamri Glacier is probably surging. This has previously been mentioned by some researchers such as Copland et al. The Equilibrium Line Altitude was found to be at about 5,000 m a.s.l for south tributaries, estimated from the surface velocity distribution along the glacier centerline.

Keywords Glacier surface velocity · SAR feature tracking · GAMMA software · Karakoram Mountains

Introduction

Mountain glaciers are sensitive indicators of climate fluctuations (Lemke et al. 2007; McCarthy et al. 2001). Most glaciers in western China have retreated to some degree with increasing precipitation and temperature during the past half century (Liu et al. 2006). The Karakoram Mountains are one of the most remote and least accessible mountain ranges in the world, where many surges have occurred historically (Hewitt 1969, 1998; Shangguan et al. 2005; Copland et al. 2009). Little is known about the behavior of the glaciers in the Karakoram Range and little fieldwork has been completed. There are no ground measurements from the Yengisogat Glacier, the largest glacier in China (Yang 1987). As temperatures continue rising there will likely be a greater number of glacier lake outburst floods (GLOFs) threatening downstream communities (Feng 1991; Shen et al. 2004). Therefore, more attention should be paid to these glaciers, with research focusing on factors such as glacier temperature and velocity fields.

Measuring glacier surface velocities can provide indicators of glacier motion change or surge and are used to

Z. Jiang · J. Lin · S. Long · Y. Han · X. Wang
Hunan Province Key Laboratory of Coal Resources
Clean-Utilization and Mine Environment Protection,
Hunan University of Science and Technology,
Xiangtan 411201, China

Z. Jiang · S. Liu (✉)
State Key Laboratory of Cryospheric Sciences,
Cold and Arid Regions Environmental and Engineering
Research Institute, Chinese Academy of Sciences,
Lanzhou 730000, China
e-mail: liusy@lzb.ac.cn

J. Peters
Institute of Cartography, Technische Universität,
Dresden, Germany

understand glacier dynamics (Berthier et al. 2005; Kääb 2005; Pritchard et al. 2005; Quincey et al. 2007). Models explain surging as a result of internal, mainly thermal and hydrological, developments affecting the base of the glacier, possibly involving soft basal sediments. It can be understood that the motion due to internal ice deformation or basal sliding by analyzing the transverse profile velocity patterns. For example, if the transverse velocity profile shows a sharp change from the glacier margin to the central part, this indicates that the glacier is experiencing basal sliding (Copland et al. 2009).

The use of satellite synthetic aperture radar (SAR) imagery has been shown to be a feasible method to measure glacier surface velocities and has advantages over other traditional methods such as ground measurements by which only point information was provided and only short time interval observations could be achieved (Gabriel et al. 1989; Goldstein et al. 1993; Kwok and Fahnestock 1996; Luckman et al. 2007; Mohr et al. 1998; Quincey et al. 2009b; Strozzi et al. 2002). SAR interferometry has been a widely used method to obtain glacier surface velocities (Gabriel et al. 1989; Goldstein et al. 1993); however, it is limited by serious decorrelation in long observation intervals for most satellites in service such as ERS (with 35 days repeat orbit) and by the fact that only deformation in the range direction can be obtained. If the glacier flow direction is far from or perpendicular to the SAR line of sight (LOS), then the motion cannot be detected (Pritchard et al. 2005; Rosen et al. 2000). SAR feature tracking can overcome these problems in retrieving three-dimensional velocities reliably and robustly (Scherler et al. 2008). This method can measure deformations in range and azimuth directions using the intensity tracking even if the SAR image pairs are incoherent (Strozzi et al. 2002).

In this study the SAR feature-tracking (SRFT) technique is used to retrieve glacier surface rates because SAR interferometry is hampered due to the lack of coherence between advanced land observing satellite (ALOS) phased array type L-band synthetic aperture radar (PALSAR) data with 46-day offsets. This method has been used to calculate the surface velocity of fast-moving glaciers such as Sortebræ Glacier in Greenland (Pritchard et al. 2005; Strozzi et al. 2002, 2008) and glaciers in the Karakoram Himalaya region (Copland et al. 2009; Luckman et al. 2007; Quincey et al. 2009a, b) with annual average velocity errors $<7 \text{ m year}^{-1}$. Surface velocities of the Yengisogat Glacier are calculated using offset tracking of ALOS PALSAR images in combination with a digital elevation model (DEM) with 90-m resolution. Then the estimated surface velocity is compared with previous results to validate the method. The seasonal surface velocity variations and spatial patterns are presented to discuss the glacier

dynamics in relation to glacier surging. The equilibrium line altitude estimated by the distribution of surface velocities along the central flow line is also discussed. Additionally, a time series of satellite optical images is compared to discuss the tributary glacier terminus change.

Study area

The Yengisogat Glacier is located in the Karakoram Mountains of western China at $\sim 36.0^\circ\text{N}$, $\sim 76.0^\circ\text{E}$. Also known as the Skamri Glacier, the Yengisogat is a mid-latitude, subpolar glacier (Shi 2000). No in situ fieldwork has been carried out for this glacier; the only data available is a topographic map obtained by aerial photogrammetry in the 1970s. This glacier was also named *crevasses glacier* (Yang 1987; Zhang 1980) because so many crevasses and seracs were observed from the aerial photos, extending almost to the snowline, which is the reason why ground measurements are impossible. The Yengisogat Valley is oriented from northwest to southeast, including four main tributaries and several small glacier flows. The glacier trunk is about 42-km-long as measured from aerial photos and occupies $\sim 379.97 \text{ km}^2$. The summit of this glacier is 7,050 m a.s.l., and the terminus is 4,000 m a.s.l. Yang and An (1989) found that the average equilibrium-line altitude (ELA) was at $\sim 5,400 \text{ m a.s.l}$ and the north tributary's ELA was at $\sim 5,500 \text{ m a.s.l}$, higher than that of south tributary at 5,380 m a.s.l (Fig. 1).

Data source and methods

Data source

The ALOS satellite was launched in early 2006, with data collected by the PALSAR sensor in the L-band ($\lambda = 23.5 \text{ cm}$). ALOS PALSAR data including fine-beam single-polarization mode (FBS) and fine-beam double-polarization mode (FBD) were collected by the Japan Aerospace Exploration Agency (JAXA). The available ALOS PALSAR data cover all four seasons within a 2-year period as Table 1 shows.

All images are in ascending orbit. All data pairs employed for SRFT have a 46-day acquisition interval between images. Data employed are single-look complex (SLC). For FBD data, HH polarization was employed because no suitable image pair was available for summer 2008; the data pair of summer 2009 was selected instead.

Four tiles of SRTM DEM Version 3 data downloaded from the website (<http://wist.echo.nasa.gov>) were used to geo-code the ALOS PALSAR imagery using GAMMA

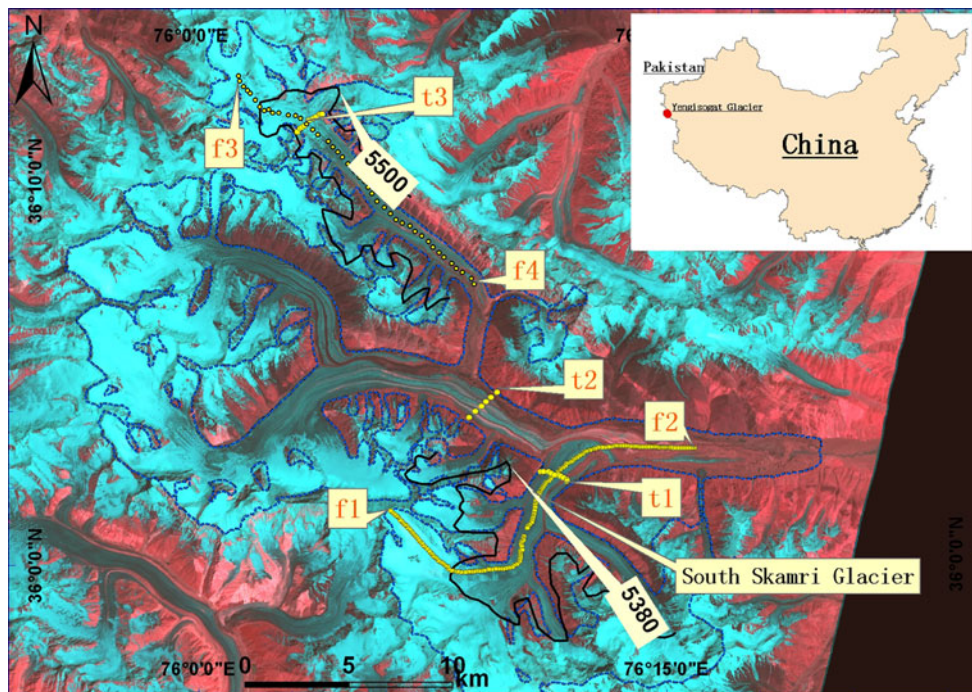


Fig. 1 Yengisogat Glacier, with profile locations (in yellow) highlighted. The red area in the inset map indicates the position of the study area. The background is Advanced Space borne Thermal Emission and Reflection Radiometer (ASTER) imagery (26-05-2007).

The blue dashed line and the black solid line were the border of the Yengisogat Glacier and equilibrium line, respectively, both from the First Chinese Glacier Inventory (Yang and An 1989)

Table 1 ALOS PALSAR scenes covering the study area and used in the application of SRFT to derive glacier surface velocity

ID	First orbit	Image date	Second orbit	Image date	Data type	Polarization
Autumn	08222	10–08–2007	08893	25–09–2007	FBD	HH
Winter	10235	26–12–2007	10906	10–02–2008	FBS	HH
Spring	10906	10–01–2008	11577	27–03–2008	FBS	HH
Summer	18287	30–06–2009	18958	15–08–2009	FBD	HH

Table 2 ASTER and MSS/TM used in this study

MSS/TM		ASTER	
ID	Date	ID	Date
LM21600350078155101	04–06–1978	ast_11a_00307262006055231	07–26–2006
P148r35_5t19900629	29–06–1990		
L71148035_03520030321	21–03–2003	ast_11a_00306272007055252	06–27–2007

software and derive the altitude, slope and aspect of the glacier surface within the ArcGIS software (ESRI). The Shuttle Radar Topographic Mission (SRTM) digital elevation model (DEM) is regarded as a precise and global elevation dataset which has been used widely before (Berthier et al. 2006; Rodríguez et al. 2001). Each tile is 1,201 × 1,201 pixels in size (1° × 1°); the pixel-posting interval is three arc-seconds, or about 90 m in horizontal direction, which is similar to the velocity map resolution

(~100 m). For FBD data steps of 6 pixels and 36 pixels are set for range and azimuth direction, respectively, while implementing offset-tracking procedures within the GAMMA software.

Also, a time series of USGS Landsat Multispectral Scanner (MSS) data, Thematic Mapper (TM) images and ASTER imagery (Table 2) collected from the USGS website (<http://glovis.usgs.gov/>) were employed to demonstrate obvious glacier flow change.

Methods

SAR feature tracking is implemented by calculating the offsets between two SAR images using offset tracking procedures within the GAMMA software. Intensity

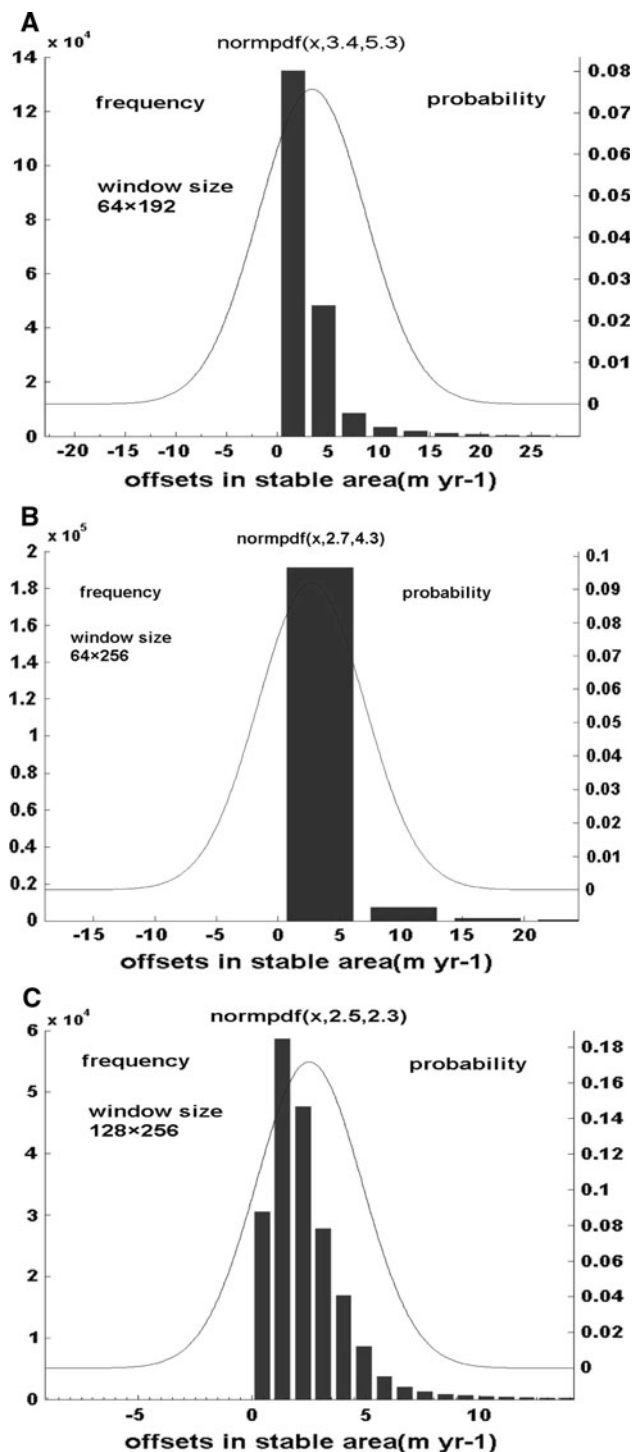


Fig. 2 Distribution of measured 46-day tracking offsets of the spring data pair over non-glacier areas and for 216,850 samples in *horizontal direction* (magnitude) using different choices of search window size

tracking and coherence tracking are often used. The intensity tracking was preferred due to the low coherence of ALOS PALSAR data pairs with 46 days offset. SAR feature tracking is performed by cross-correlating samples of two SAR images with global offset (which is the offset between the image pairs due to the orbital difference). The global offset is determined by fitting a polynomial to the offsets of relatively few, distributed static points (Pritchard et al. 2005). The processing chain includes (1) coarse offset estimation using the orbital data file. (2) The fine offset estimation using intensity cross correlation. (3) The fine estimated offsets of two PALSAR images were then used to generate offsets with global offsets removed in both ground range and azimuth directions and employed to calculate the displacement of the glacier's surface (Pritchard et al. 2005; Strozzi et al. 2002). The estimated offsets are unambiguous values, which means there is no need for phase unwrapping.

In this study horizontal offsets in the radar geometry were extracted from the data pairs using the GAMMA software. The obtained range and azimuth offset were used to calculate the glacier motion direction. The shadow and layover areas were rejected and areas with slope angles greater than 20° were also masked out (Quincey et al. 2009b). Some abnormal values from the original results of offset-tracking processing can be filtered using methods described by Dwyer (Berthier et al. 2005; Dwyer 1995). For example, over a 5×5 neighborhood vectors varying by more than 45° from the mean direction, or 3.5 times the interquartile range from the median magnitude, were rejected (Pritchard et al. 2005).

The three-dimensional surface velocity V_f is calculated using the following formula:

$$V_f = \frac{V_h}{t \times \cos \alpha} \quad (1)$$

where V_h is the horizontal offset in geographic coordinates, α is the glacier surface slope (glacier flows were presumed to occur along maximum slope direction) and t is the data pair acquisition time interval.

In this work seasonal velocity fields were obtained and the average annual velocity was computed based on the four seasonal measurements.

Table 3 Errors of SRFT with 128×256 window size searching

ID	Data pairs		Theoretical errors (m year ⁻¹)	Errors in stable areas (m year ⁻¹)
	First orbit	Second orbit		
Autumn	08222	08893	3.65	5.01
Winter	10235	10906	8.03	11.50
Spring	10906	11577	2.92	2.3
Summer	18287	18958	2.55	5.55

Errors and uncertainties

The main errors are related to the co-registration, transformation of offset to surface flow velocity and systematic errors (Nakamura et al. 2007; Strozzì et al. 2002, 2008). The

theoretical error of offset in the horizontal direction caused by co-registration is shown in the following equation:

$$\delta_h = \frac{2(R \times \Delta R + A \times \Delta A)}{\sqrt{R^2 + A^2}} \quad (2)$$

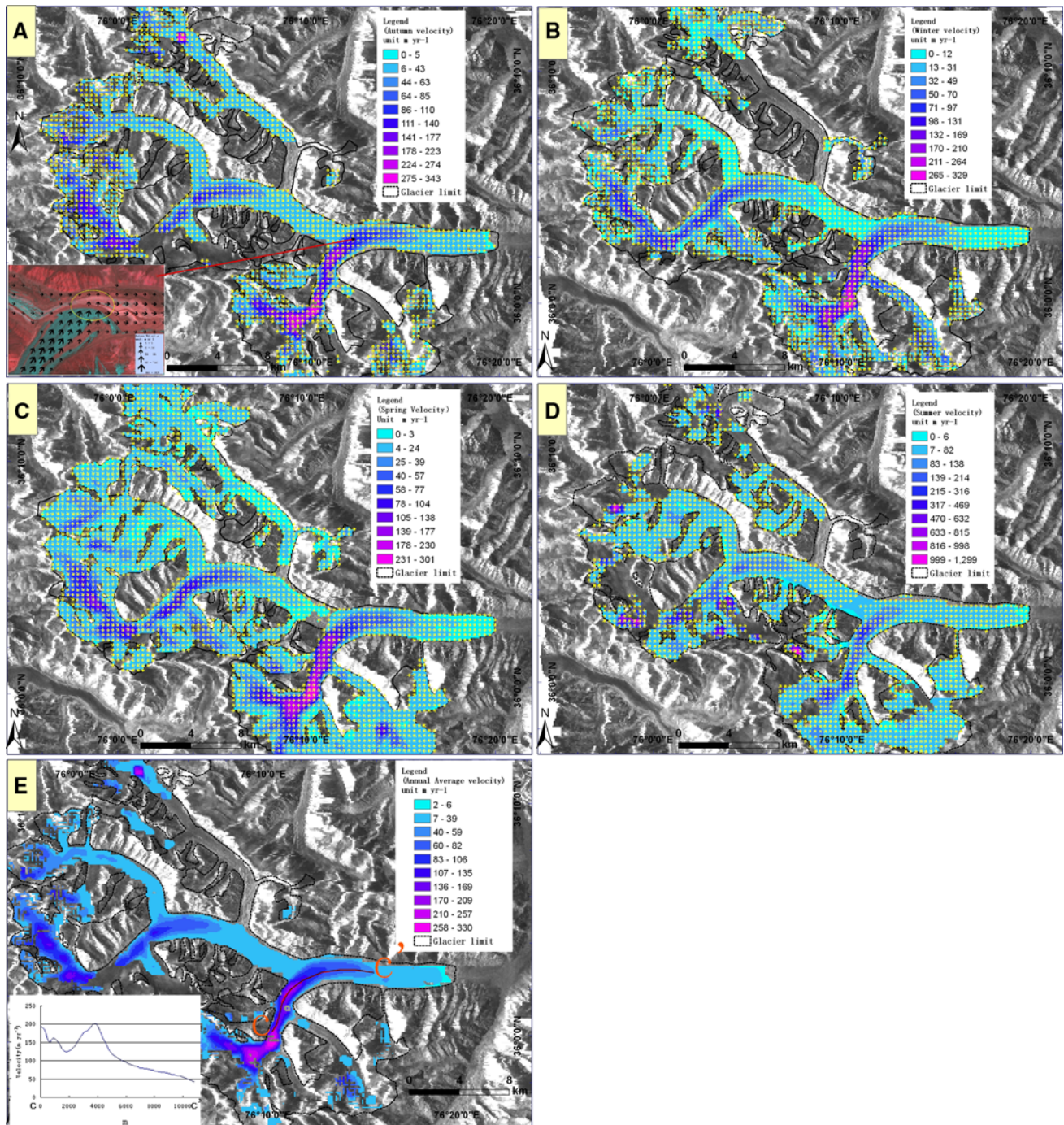


Fig. 3 The glacier seasonal and annual average surface velocity fields from SRFT. Velocities were not shown where they were less than the errors estimated in each image pair or failed tracking, as mentioned in Table 3. For the sake of convenience, SRFT results were also identified by the acquisition time: autumn is represented by

the 10 August 2007 and 25 September 2007 data pair (a); winter by the 26 December 2007 and 10 February 2008 data pair (b); spring by the 10 February 2008 and 27 March 2008 data pair (c); and summer by the 30 June 2009 and 15 August 2009 data pair (d)

where δ_h is the theoretical error in the horizontal direction, R is the offset measured in the Radar range direction, A is the offset measured in the Radar azimuth direction; ΔR is the standard deviation of co-registration in the range direction and ΔA is the standard deviation of co-registration in the azimuth direction.

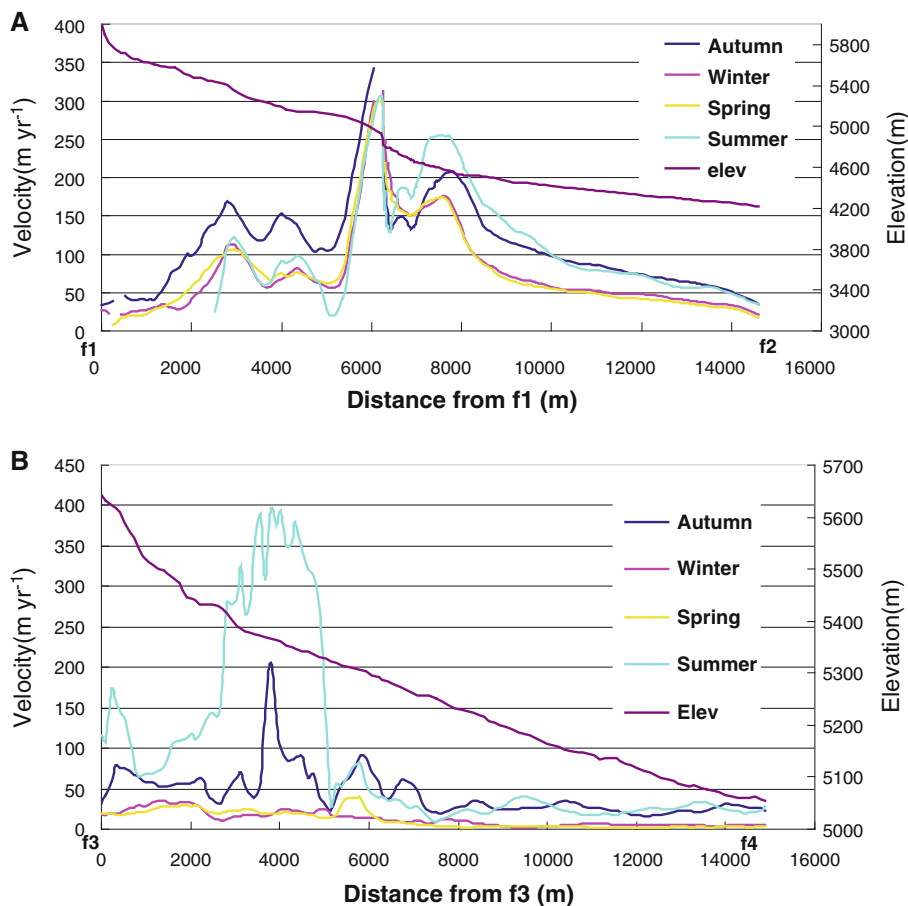
The theoretical errors are larger than 1.414 times the sum of the range and azimuth errors, and less than 2 times the range or azimuth errors from above Eq. (2), which is strongly dependent on the orientation of the glacier relative to the SAR imaging geometry. Therefore, the theoretical error in horizontal direction is roughly the sum of the range and azimuth errors (Strozzi et al. 2002). This method was applied to estimate the theoretical errors of SRFT. The errors include the systematic noise and the ionospheric effects, which could be regarded as a constant while testing the stable area (Pritchard et al. 2005; Strozzi et al. 2002; Werner et al. 2005). Static areas such as non-glaciated regions (e.g., rocks) and areas >100 m distance away from rivers were tested to provide the total errors in this research.

SAR feature tracking is a feasible method to measure glacier surface flow but still has some uncertainties. For example, there is an uncertainty about the offset estimation

between two images due to the different set size of the search window when offset-tracking procedures were implemented. Generally, the size of the search window should not be less than the estimated offset caused by glacier motion. Pritchard et al. (2005) found that a search window size of 64×256 pixels would double the number of successful matches of 64×64 chips for fast-moving glaciers in Greenland (Pritchard et al. 2005; Strozzi et al. 2002). For all glaciers investigated in the Karakoram Mountains, the 128×256 search chips of ALOS PALSAR FBD data corresponding to $\sim 2,000$ m in range and ~ 800 m in azimuth direction were sufficient for successful tracking (Fig. 2). The relatively larger window size is necessary to capture sufficient ground features in the presence of image speckle and may result in a degree of smoothing of the displacement fields (Quincey et al. 2009a).

Comparing velocity errors computed for stable areas using different window sizes (Fig. 2a–c), it is found that the mean is 3.4 m year^{-1} and SD is 5.3 m year^{-1} using a 64×192 window size; mean is 2.7 m year^{-1} and SD is 4.3 m year^{-1} using a 64×256 window size; Mean is 2.5 m year^{-1} and SD is 2.3 m year^{-1} using a 128×256 window size. Therefore, the 128×256 window size was

Fig. 4 Seasonal and spatial variation of the glacier surface velocities along center line



chosen. The SD value is quoted as the true error for the spring data pair. The true errors of other seasonal image pairs were calculated in the same way. For ALOS PALSAR FBS data and FBD data the errors in horizontal direction are listed in Table 3.

The theoretical errors in Table 3 are roughly computed using the method referred to above. For example, the theoretical value of errors to the Autumn pair is 3.65 m year^{-1} , which was calculated by $9.368 \times 0.017 + 3.153 \times 0.085 \approx 0.43 \text{ m}$ in 46 days (equivalent to 3.65 m year^{-1}) (the pixel size of ALOS PALSAR FBD data is 9.368 and 3.153 m in range and azimuth direction, respectively). The standard deviation of the final polynomial model fit in range and azimuth direction is 0.017 and 0.085, respectively). The other pairs' relative *theoretical* errors were also estimated by this method. The errors of annual average velocity are $\sim 6.27 \text{ m year}^{-1}$, computed by the average of errors of four measurements. The error in stable areas was regarded as the true errors.

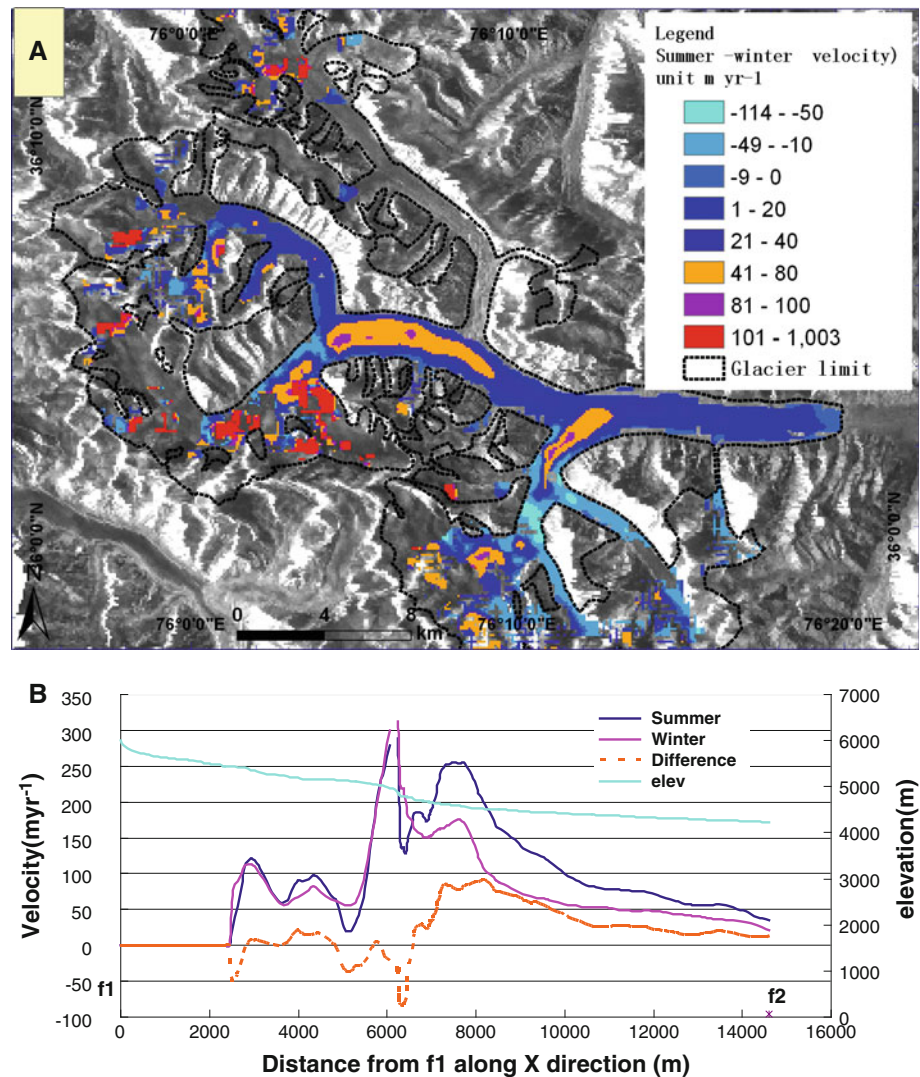
The true errors of data pairs in winter were much larger than that of any other pair due to more theoretical errors of offset estimation (Table 3) between two images employed which is caused by the quality of the ALOS PALSAR data used.

As discussed above, glacier surface flow was assumed to be parallel to the glacier surface along the slope gradient direction. This assumption may introduce some errors. Generally speaking, glaciers do not flow parallel to the surface; in fact, glacier flow is inclined slightly upwards in the ablation zone and slightly downwards in the accumulation zone (Paterson 1994).

Results

The following figures (Fig. 3a–e) revealed the seasonal velocity distribution and spatial variation of the valley glacier.

Fig. 5 Surface velocities difference between summer and winter



Comparing the velocity distributions in each figure (Fig. 3a–e), it was shown that the south tributaries were moving faster than north tributaries and that two south tributaries almost dominated the main flow in each observed time interval. This may be attributed to the glacier's aspect. From a long-term point of view the glacier's orientation has an important role in glacier development. The northern tributary in the valley that received more solar radiations would retreat much more than the southern tributaries. This leads to the slowing down flow due to less mass. The average annual velocity of South Skamri Glacier was in agreement with previous work undertaken here using feature tracking with optical imagery (Copland et al. 2009). When comparing velocities along the central flow line C–C' with previous results (Copland et al. 2009, their Fig. 3a), some differences existed and the annual average surface velocity from SRFT was slightly lower than that from optical imagery feature tracking. This was probably due to the different acquisition dates of the two data sets (ALOS PALSAR data were obtained in 2007–2008; ASTER in 2006–2007; Copland et al. 2009).

Discussion

Seasonal and spatial variation

The following figures show the comparison of the glacier's seasonal (Fig. 4a, b) and spatial (Fig. 5a, b) surface velocity.

The seasonal glacier surface velocity fields from SRFT and corresponding velocity distributions along the central flow lines f1–f2' and f3–f4'; the Velocity unit is meters per year (m year^{-1}); the red solid lines f1–f2' and f3–f4' are the central flow lines of tributaries (all profiles are labeled in Fig. 1).

The velocities in summer were obviously higher than in winter below 5,000 m a.s.l., while similar above 5,000 m a.s.l. There also existed some sections where winter velocity was higher than summer. This may be caused by more snow accumulation in winter in the upper part of the glacier or the occurrence of more tracking errors in the snow-covered area.

Moreover, it shows that the elevation of the surface velocity peak is about 5,000 m a.s.l in the seasonal or annual average surface velocity maps (Fig. 4), which is lower than the equilibrium line altitude [ELA $\sim 5,380$ m a.s.l (Yang and An 1989)]. Theoretically speaking, the velocity around the ELA reaches its maximum of the glacier length according to glacier dynamics (Paterson 1994). Since this is a glacier with complex glacier flow and the presence of surging, it is hard to find the ELA using surface velocity distribution alone. Other parameters such as

surface mass balance, glacier thickness and slope should therefore be obtained to estimate the ELA.

Basal sliding versus internal deformation

Comparison of the spatial and seasonal glacier surface velocities (Fig. 3a–e) along the center lines f1–f2 and f3–f4 shows that the summer and autumn velocities were faster than in spring and winter along the flow line f3–f4 and summer velocity was ten times that of winter velocity in comparison with the summit values of these seasons. This implies that it might be moving fast or surging in summer.

It is clear that the transverse surface velocities follow the principle that velocities at a glacier's center flow line are the maximum and decrease toward the margins. The surface velocities in summer were faster than that of the other seasons and increased rapidly from glacier margin to glacier center in each transverse profile (Fig. 6a). This implies 'block flow' due to basal sliding and that it was probable surging in that period. In comparison, the velocity

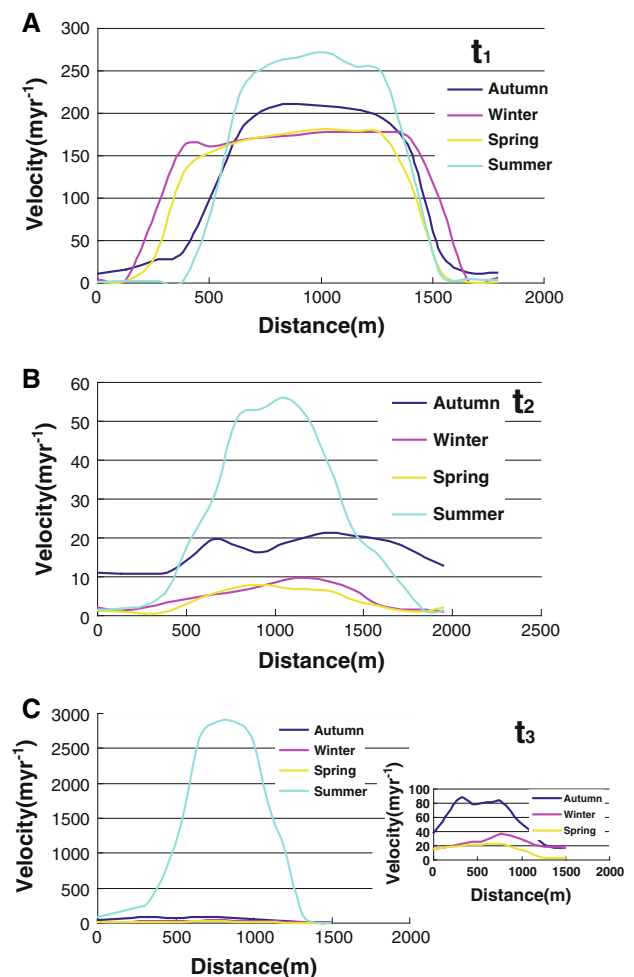


Fig. 6 Comparison of seasonal surface velocity change along transverse profile t_1 t_2 and t_3

in other seasons along the transverse profiles increased gently. The summer velocity was about 250 m year^{-1} in transverse t1, which was consistent with the previous measurements using optical imagery feature tracking (Copland et al. 2009 Fig. 3a). Judging from the inset in Fig. 3a, the ice motion directions were not consistent with the surface flow features near the medial moraines in the ellipse area (Fig. 3a), being almost perpendicular to the surface flow features. This indicates that the South Skamri Glacier is moving forward and still pushing into the glacier trunk. For transverse profile t2 (Fig. 6b) the summer velocity is much faster than in other seasons, but the velocity value is relatively smaller compared with the other transverse profiles. For transverse profile t3 on the north tributary the summer velocity is far more rapid than in any other season. This might be due to the fast motion of the glacier, avalanche or due to feature tracking error caused by snow cover.

The southern tributaries may be moving faster than northern and might surge in summer based on the above analysis. Following (Fig. 7a–d) a time series of satellite images is presented to illustrate this phenomenon.

The time series of optical images (Fig. 7a–d) shows that the South Skamri glacier terminus (M location) moved forward a few hundred meters from 1978 to 1990. This indicates that it had surged over that time. It still moved forward between 1990 and 2007, which implies that South Skamri terminus is still pushing the trunk. The terminus of a small tributary (N location) adjacent to it was moving forward throughout those years. The front of tributary N has extended into the main glacier body near its terminus. Probably the little tributary had surged too, although more work should be done to prove it.

As mentioned by some literature (Hewitt 1969, 2005), glaciers in the Karakoram Mountains have an anomaly in behaviors such as surge or terminus advancing while most glaciers in the world are experiencing recession. For example, rapid declines are reported throughout the Greater Himalaya and most of mainland Asia. These trends have been attributed to global atmospheric warming. From the 1920s to the early 1990s most glaciers of the Karakoram were also observed to diminish, except for some short-term advances in the 1970s. However, in the late 1990s any central Karakoram glaciers began expanding (Hewitt 2005).

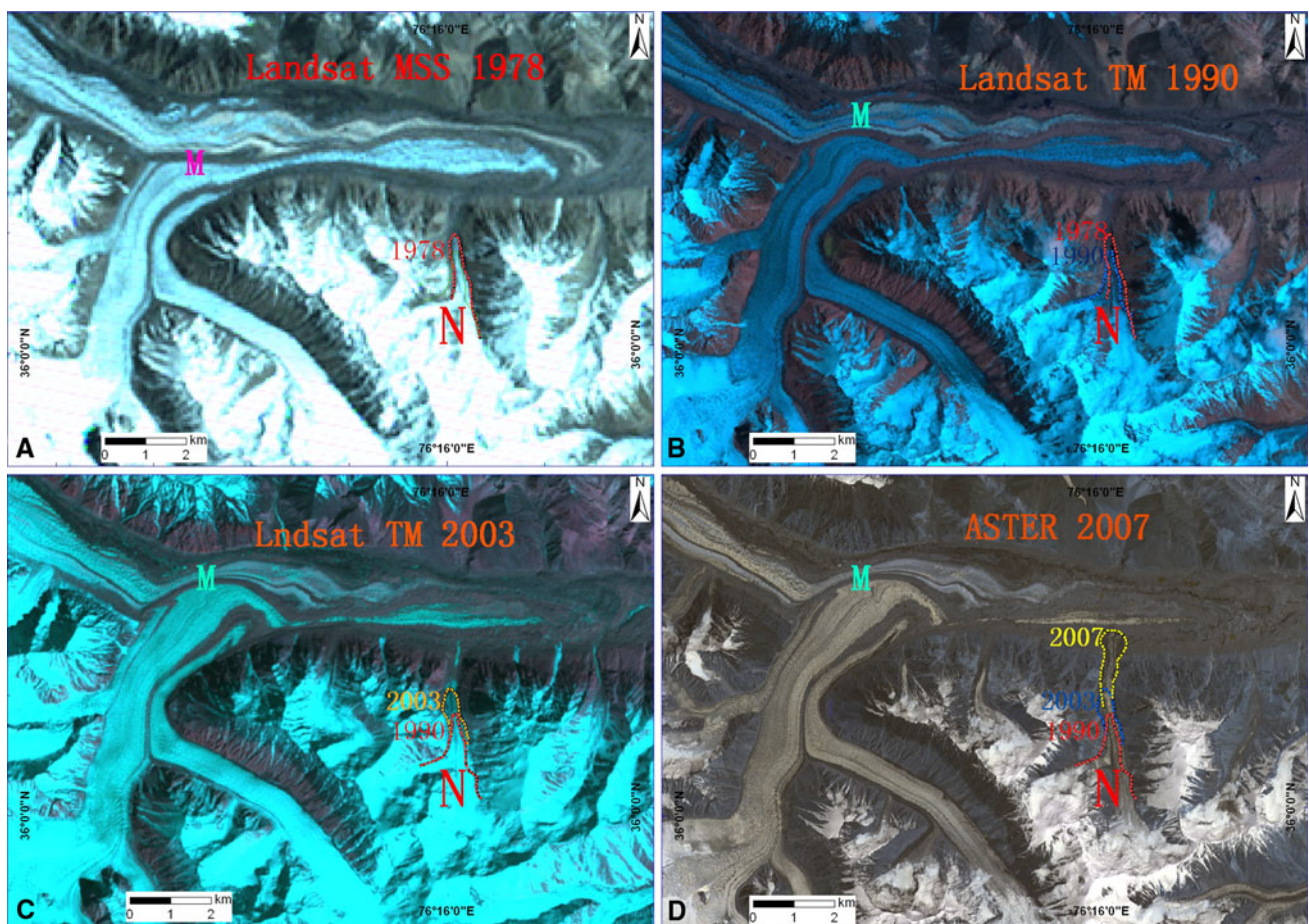


Fig. 7 A time series of ASTER and TM/MSS images to illustrate the frontal change of the tributaries

This may be attributed to precipitation increasing over the Karakoram region. There have been statistically significant increases in winter, in summer and in the annual precipitation at several climate stations over this region since 1961 (Archer and Fowler 2004). This may have led to positive mass balances, which made the glacier terminus advancing or surging.

Conclusions

SAR feature tracking is a feasible method to retrieve glacier surface flow velocities, especially for cloud- and snow-covered areas where visible optical images do not work well. SAR feature tracking can measure glaciers' surface velocity over long acquisition time intervals and the results match fairly well with a previous study using optical imagery feature tracking. As the results discussed above show, the southern tributaries of the Yengisogat Glacier were moving faster than the northern tributaries. In addition, the South Skamri Glacier is moving rapidly or surging based on the transverse (t_1) velocity distribution and difference between the ice motion direction and surface flow features near the front of South Skamri Glacier.

Acknowledgments This work was funded by the Innovation Project of Chinese Academy Sciences (KZCX2-YW-Q03-04); the National Natural Science Foundation of China (No. 1141071044) and the National Basic Work Program of Chinese MST (Glacier Inventory of China II, Grant No. 2006FY110200) and National Natural Science Foundation of China (No. 41004002) and Project for Incubation of Specialists in Glaciology and Geocryology of National Natural Science Foundation of China (No. J0930003/J0109). The authors thank Dr. Elizabeth Susan Garcia for editing and modifying the manuscript and appreciate the reviewers very much for their useful comments and suggestions.

References

- Archer DR, Fowler HJ (2004) Spatial and temporal variations in precipitation in the Upper Indus Basin, global teleconnections and hydrological implications. *Hydrol Earth Syst Sci* 8:47–61
- Berthier E, Arnaud Y, Vincent C, Remy F (2006) Biases of SRTM in high-mountain areas: Implications for the monitoring of glacier volume changes. *Geophys Res Lett* 33:1–8
- Berthier E, Vadonb H, Baratouxc D, Arnaudd Y, C. Vincente, Feigl KL, Rémya F, Legrésya B (2005) Surface motion of mountain glaciers derived from satellite optical imagery. *Remote Sens Environ*, pp 14–28
- Copland L, Pope S, Bishop MP, Shroder JF Jr, Clendon P, Bush A, Kamp U, Seong YB, Owen LA (2009) Glacier velocities across the central Karakoram. *Ann Glaciol* 50:41–49
- Dwyer JL (1995) Mapping tide-water glacier dynamics in East Greenland using Landsat data. *J Glaciol* 41:584–595
- Feng Q (1991) Characteristics of Glacier Outburst Flood in the Yarkant River, Karakorum Mountains. *GooJournal* 25:255–263
- Gabriel AK, Goldstein RM, Zebker HA (1989) Mapping small elevation changes over large areas: differential radar interferometry. *J Geophys Res* 94(B7):9183–9191. doi: 10.1029/JB094iB07p09183
- Goldstein RM, Engelhardt H, Kamb B (1993) Satellite radar interferometry for monitoring ice sheet motion: application to an Antarctic ice stream. *Science* 262:1525–1530
- Hewitt K (1969) Glacier surges in the Karakoram Himalaya (Central Asia). *Can J Earth Sci* 6:1009–1018
- Hewitt K (1998) Glaciers receive a surge of attention in the Karakoram Himalaya. *Eos Trans* 79:104
- Hewitt K (2005) The Karakoram Anomaly? Glacier expansion and the 'elevation effect', Karakoram Himalaya. *Mt Res Dev* 25:332–340
- Kääb A (2005) Combination of SRTM3 and repeat ASTER data for deriving alpine glacier flow velocities in the Bhutan Himalaya. *Remote Sens Environ* 94:463–474
- Kwok R, Fahnestock MA (1996) Ice sheet motion and topography from radar interferometry. *IEEE Trans Geosci Remote Sens* 34:189–200
- Lemke P, Ren J, Alley RB, Allison I, Carrasco J, Flato G, Fujii Y, Kaser G, Mote P, Thomas RH, Zhang T (2007) Observations: changes in snow, ice and frozen ground. In: Solomon S, Qin D, Manning M, Chen Z, Marquis M, Averyt KB, Tignor M, Miller HL (eds) *Climate change 2007: the physical science basis. Contribution of working group I to the fourth assessment report of the intergovernmental panel on climate change*. Cambridge University Press, Cambridge
- Liu S, Ding Y, Li J, Shangguan D, Zhang Y (2006) Glaciers in response to recent climate warming in western China. *Quat Sci* 26:762–771 (summary in Chinese)
- Luckman A, Quincey D, Bevan S (2007) The potential of satellite radar interferometry and feature tracking for monitoring flow rates of Himalayan glaciers. *Remote Sens Environ* 111:172–181
- McCarthy JJ, Canziani OF, Leary NA, Dokken DJ, White KS (2001) Contribution of working group II to the third assessment report of the intergovernmental panel on climate change (IPCC). Cambridge University Press, UK
- Mohr JJ, Reeh N, Madsen SN (1998) Three-dimensional glacial flow and surface elevation measured with radar interferometry. *Nature* 391:273–276
- Nakamura K, Doi K, Shibuya K (2007) Estimation of seasonal changes in the flow of Shirase Glacier using JERS-1/SAR image correlation. *Polar Sci* 1:73–83
- Paterson WSB (1994) *The physics of glaciers*, 3rd edn. Elsevier, Oxford, pp 1–480
- Pritchard H, Murray T, Luckman A, Strozzi T, Barr S (2005) Glacier surge dynamics of Sortebrae, east Greenland, from synthetic aperture radar feature tracking. *J Geophys Res* 110:1–13
- Quincey DJ, Richardson SD, Luckman A, Lucas RM, Reynolds JM, Hambrey MJ, Glasser NF (2007) Early recognition of glacial lake hazards in the Himalaya using remote sensing datasets. *Glob Planet Chang* 56:137–152
- Quincey DJ, Copland L, Mayer C, Bishop M, Luckman A, Belo M (2009a) Ice velocity and climate variations for Baltoro Glacier, Pakistan. *J Glaciol* 54:1061–1071
- Quincey DJ, Luckman A, Benn D (2009b) Quantification of Everest region glacier velocities between 1992 and 2002, using satellite radar interferometry and feature tracking. *J Glaciol* 55:596–606
- Rodríguez E, Morris CS, Belz JE, Chapin EC, Martin JM, Daffer W, Hensley S (2001) *An Assessment of the SRTM Topographic Products*. JPL
- Rosen PA, Hensley S, Joughin IR, Li FK, Madsen SRN, Rodriguez E, Goldstein RM (2000) Synthetic aperture radar interferometry. In: *Proceedings of the IEEE*, pp 333–382
- Scherler D, Leprince S, Strecker MR (2008) Glacier-surface velocities in alpine terrain from optical satellite imagery—accuracy

- improvement and quality assessment. *Remote Sens Environ* 112(10):3806–3819
- Shangguan D, Shiyin L, Yongjian D, Lianfu D, Yongping S, Anxin L, Gang L, Yong Z, Changwei X (2005) Surging glacier found in Shaksgam River, Karakorum Mountains. *J Glaciol Geocryol* 5:642–644 (summary in Chinese)
- Shen Y, Ding Y, Liu S, Wang S (2004) An increasing glacial lake outburst flood in Yarkant River, Karakorum in past ten years. *J Glaciol Geocryol* 26(2):234
- Shi Y (2000) Glacier and their environmentals in China—the present, past and future. Science Press, Beijing (summary in Chinese)
- Strozzi T, Luckman A, Murray T, Wegmüller U, Werner CL (2002) Glacier motion estimation using SAR offset-tracking procedures. *IEEE Trans Geosci Remote Sens* 40:2384–2391
- Strozzi T, Kouraev A, Wiesmann A, Wegmüller U, Sharov A, Werner C (2008) Estimation of Arctic glacier motion with satellite L-band SAR data. *Remote Sens Environ* 112:63–645
- Werner C, Wegmüller U, Strozzi T, Wiesmann A (2005) Precision estimation of local offsets between pairs of SAR SLCs and detected SAR images. IGARSS'05, Seoul
- Yang H (1987) General characteristics of the Yinsugaiti Glacier. *J Glaciol Geocryol* 9:97–98 (summary in Chinese)
- Yang H, An R (1989) Glacier inventory of China-Yarkant River. Science Press, Beijing (summary in Chinese)
- Zhang X (1980) Recent variations of the Insukati Gacier and adjacent glaciers in the Karakoram Mountains. *J Glaciol Geocryol* 3:12–16 (summary in Chinese)